



Chitosan's Structural Properties which Extracted from Marine Crustacean

N.Annlin Bezy¹, S.Jasvy¹, S.Virgin Jeba² and A.Lesly Fathima^{2*}

¹Research Scholar (Reg. No. 20213042132006), Department of Physics, Holy Cross College, Nagercoil, (Affiliated to Manonmaniam Sundaranar University, Tirunelveli), Tamil Nadu, India.

²Assistant Professor, Department of Physics, Holy Cross College, Nagercoil (Affiliated to Manonmaniam Sundaranar University, Tirunelveli), Tamil Nadu, India.

Received: 25 Aug 2023

Revised: 20 Sep 2023

Accepted: 22 Nov 2023

*Address for Correspondence

A.Lesly Fathima

Assistant Professor,

Department of Physics,

Holy Cross College, Nagercoil

(Affiliated to Manonmaniam Sundaranar University, Tirunelveli),

Tamil Nadu, India.

E.mail: leslysat@gmail.com



This is an Open Access Journal / article distributed under the terms of the **Creative Commons Attribution License** (CC BY-NC-ND 3.0) which permits unrestricted use, distribution, and reproduction in any medium, provided the original work is properly cited. All rights reserved.

ABSTRACT

Chitosan, a polysaccharide derived from shells including crab, lobster, fish scales, and shrimp, is being used to produce improved products in paint, food, agriculture, textile industries, and in water treatment. This study's goal is to improve chitosan's capacity to meet the demands in diverse fields. Chitosan is extracted by undergoing demineralizing, deproteinizing, and deacetylating of fresh shrimp shell that has been harvested locally. The FTIR and XRD measurements are made to confirm the isolated material is chitosan. The NH stretching and amide group is the major bond in chitosan and is observed in the taken FTIR. The SEM reveals the morphology of obtained chitosan has uniform-sized porous. The extracted chitosan can be utilized for both home and industrial purposes, including filters, energy storage, medicine administration, etc., because of the porosity distributed over its surface. Chitosan's photoluminescence emission is found in 594 nm, which comes under the green shift region. In EDAX elements Carbon, Nitrogen, and Oxygen are detected that form the polysaccharide chain chitosan. Thus, the chitosan was successfully extracted with improved morphology from shrimp shells by eliminating the calcium and protein contents.

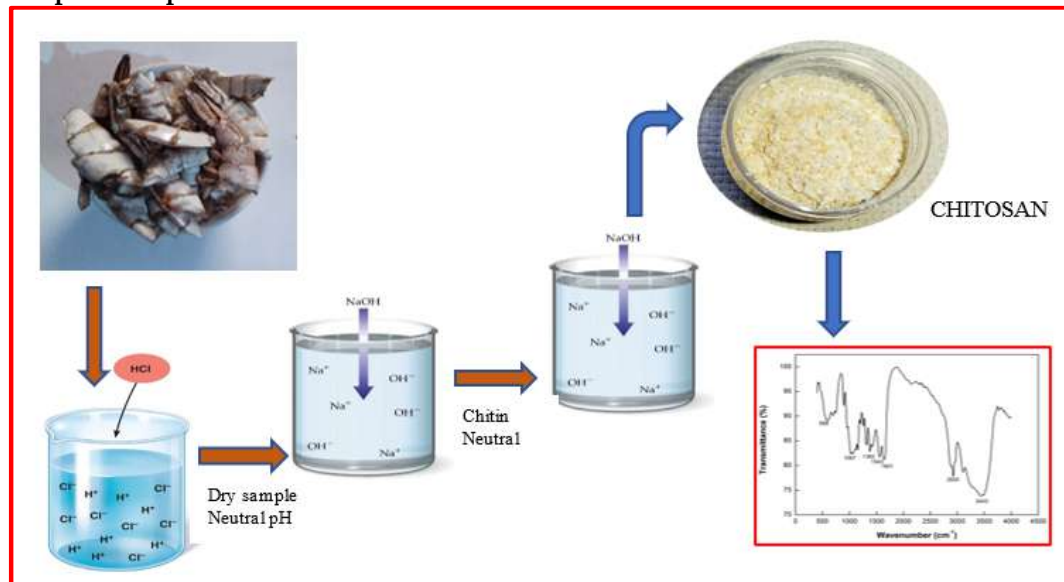
Keywords: Shrimp shell, Fourier Transform Infrared, Scanning Electron Microscopy, Filtration, Porous





Annlin Bezy et al.,

Graphical Representation



INTRODUCTION

Recently, researchers have focused on environmentally friendly biodegradable nontoxic polymers like cellulose, chitosan, etc. to improve the capacity of their role in diverse applications. Meanwhile, the current research seeks attention to generating materials that are cost-effective, straightforward in process, non-toxic, controlled-release, and biocompatible. In a similar vein, the current chitosan has various drawbacks and requires modification in adsorption, drug delivery, and other areas. Chitosan is a biopolymer that can be found in a variety of organisms, including fungi, prawns, shrimp, and arthropods. Approximately 80,000 to 100,000 tonnes of chitin from shellfish waste are produced annually in India. In this work, shrimp shells from trash are considered to be the source for the extraction of chitosan. (Bhullar et al., 2021). Chitin is converted into chitosan through the alkaline deacetylation process. Chitosan's solubility is a pivotal element considered for numerous different applications since it has a wealth of benefits when dissolved in concentrated inorganic acids like hydrochloric acid, phosphoric acid, and sulfuric acid. Chitosan has the benefit of being workable in a variety of forms, including gels, nanofibers, micro/nanoparticles, scaffolds, powder, etc. Each form can be modified in terms of structure and formation, such as film, foam, and powder, and each has a specific purpose as an adsorbent, filter membrane, or medication. (Deepthi et al., 2016). However, getting bioavailable, non-toxic chitosan with enhanced properties in a cost-effective manner has greater demand.

MATERIALS AND METHODS

The local seafood processing business provided the waste shrimp shells. It is essential to acquire from Sigma Aldrich the chemicals HCl, NaOH, and ethanol for the treatment process. Demineralization, deproteinization, and deacetylation are the three steps of the approach chosen for chemically extracting chitosan. The shrimp shell was first thoroughly cleaned in distilled water to get rid of existing any flesh and pollutants. Then it was dried and ground into powder for chemical treatments. Demineralization: Calcium carbonate and calcium phosphate mineral





Annlin Bezy et al.,

components found in the exoskeleton of crustaceans, were removed through demineralization using HCl acid. The next step is washing with distilled water to reach the pH-neutral on the treated sample.

Deproteinization: Then in deproteinization, proteins were neutralized by the treatment in diluted NaOH solution. Again, the sample was washed with distilled water until reaching the pH was neutral. After the two steps process a sample obtained is chitin. Chitin is a linear polymer chain with $\beta(1,4)$ -N-acetylglucosamine. For decolorization, the Chitin is treated in ethanol an organic solvent.

Deacetylation: Deacetylation is a vital step in the extraction of chitosan. The degree of deacetylation and molecular weight are crucial factors affected during the deacetylation stage. The chitin is deacetylated using the intense alkaline treatment of NaOH at high temperatures. Chitin's acetyl group will be eliminated with sodium hydroxide resulting in the polymer chitosan. The obtained chitosan is rinsed in distilled water to achieve a pH of neutrality before being dried and ground into powder for analysis.

CHARACTERIZATION TECHNIQUES

X-Ray Diffraction

From X-Ray Diffraction, the physical characteristics of the extracted chitosan were investigated. $\text{CuK}\alpha$ radiation with a wavelength of 1.5406\AA was used in the X'pert Pro Diffractometer with 40 kV and 30 mA of current.

Fourier Transform Infrared Spectroscopy

Fourier Transform Infrared Spectroscopy is a technique that can be used to examine the functional groups in the polymer chain. Fourier Transform Infrared Spectroscopy was performed using a SHIMADZU type IR Affinity - 1 (FTIR spectrophotometer) with a resolution of 4 cm^{-1} and in transmittance mode.

Scanning Electron Microscopy and Energy Dispersive Analysis Of X

The sample is scanned with a focussed electron beam in scanning electron microscopy, which produces a picture showing the material's topography. The ZEISS model multiSEM 505 was used to examine the chitosan's surface morphology in the micrometer range.

Photoluminescence

The optical properties of the produced carbon material were investigated using photoluminescence. The photoluminescence spectrometer (Cary Eclipse) uses a xenon flash lamp as its excitation source, and it collects emission spectra at a scan rate of 600 nm per minute.

RESULT AND DISCUSSION

X-Ray Diffraction

Figure 1 shows the obtained chitosan's XRD pattern. Broad diffraction peaks at 10 and 20 degrees seen in the XRD pattern of chitosan are its characteristics peak and some other additional peaks were also discovered. (Arafat A et al., 2015; Dokhaee et al., 2019). The amorphous form of the produced chitosan is revealed by the peak intensity. The Debye Scherrer formula, $d = k\lambda / (\beta \cos\theta)$, is used to determine the obtained chitosan grain size. In this formula, k is the Scherrer's constant of 0.9, λ is the wavelength of X-ray used at 1.5406\AA , β is the full-width half maximum, and θ is the angle of diffraction. As by formula, the calculated chitosan's average grain size is 6.09 nm. Table 1 contains the extracted chitosan's XRD data

Fourier Transform Infrared Spectroscopy

Figure 2 depicts the FTIR spectrum of the extracted chitosan from shrimp shells. The produced chitosan's FTIR peaks observed at 3443 cm^{-1} , 2925 cm^{-1} , 1651 cm^{-1} , 1543 cm^{-1} , 1382 cm^{-1} , 1067 cm^{-1} , and 599 cm^{-1} are identical to the spectra





Annlin Bezy et al.,

previously reported in (Kumari et al., 2017). The strong band at 2925cm^{-1} is caused by O-H stretching, while the peak at 3443cm^{-1} is caused by the stretching vibration of NH contained in the structure of chitosan.

To confirm the produced has chitosan high level of deacetylation, observed the weak band in 1651cm^{-1} was allocated for the amide group vibration mode, and 1543cm^{-1} is due to NH_2 bending vibration in the amino group. The C-O-H bond is represented by the presence of a band at 1382cm^{-1} , and the stretching of the C-O bond is due to the peak at 1067cm^{-1} . The peak with maximum transmittance was found at 599cm^{-1} corresponds to the glycosidic bond of CH vibration. The characteristic peak of chitosan was observed at 3443cm^{-1} and 1651cm^{-1} (Baxter et al., 1992; de Alvarenga, 2011). The other researcher including (Sagheer et al., 2009; Singh & Chahar, 2021; Trung et al., 2006; Younes et al. 2014) holds evidence of the FTIR spectrum observed in the extracted chitosan.

Scanning Electron Microscopy and Energy Dispersive Analysis Of X

Chitosan extracted from shrimp shells is observed using scanning electron microscopy (SEM) in $1\mu\text{m}$ and $0.5\mu\text{m}$ resolutions. The result shows the surface with scaffold structure distribution (Singh & Chahar, 2021). It was also found that the scaffold surface had a micro-sized interconnected porosity of rhombus shape. All of the porous membranes looked to have agglomerated fibers and rhombic forms (Thein-Han et al., 2009). The benefit of having an even scaffold is that it may have better mechanical properties, biocompatibility, and biodegradability. It may also have desired porosity for the absorbance of dyes, impurity removal, and drug delivery. Figure 3 provides the chitosan SEM images.

In EDAX, the elemental data in extracted material was evaluated. The components in the isolated chitosan are shown in Table 2. and figure 4 displays the obtained chitosan EDAX spectrum. The major and minor elements can be detected by EDAX at all levels (Nasrazadani & Hassani, 2016). The result obtained from element analysis of the extracted chitosan shows it contains carbon, oxygen, and nitrogen content.

Particle Size Distribution

An essential analysis that provides application-specific quality-related information is the particle size distribution. The particle size distribution is influenced by a material's flow, solubility, reactivity, and compressibility (Wang et al., 2021; Xu, 2015). Although there are other methods now in use to determine the particle size distribution, Dynamic Light Scattering (DLS), also known as photon correlation spectroscopy, is a useful technique. The DLS uses a laser beam's doppler shift and Brownian motion to quantify the size and dispersion of particles. Here, tools from the Malvern Zetasizer series are used to quantify particle size. DLS can be used to predict the haphazard movement of particles floating in a liquid media. The Stokes-Einstein equation's diffusion coefficient (D_t), which is used to calculate the hydrodynamic diameter (D_H) of the particles, can be used to determine the velocity /of the larger particle, which can have a low and slower Brownian motion (Sakho et al., 2017). DLS has the benefit of being automated and having a rapid measurement time while determining particle size.

Generally, D_H and D_t differ significantly depending on the size of the ions in the medium as well as the physical size of the material, particle behavior such as viscosity or diffusion, surface assembly, and texture. The particle form will alter the hydrodynamic diameter, which in turn impacts the diffusion velocity. Dynamic Light Scattering (DLS) measurements give the chitosan particle size as 6537nm in diameter. The aggregation of particles in the material with lower velocities in the medium may be the cause for the huge particle size. (Bantz et al., 2014; Ross Hallett, 1994).

Photoluminescence

Due to its great sensitivity and ability to produce images with clarity, photoluminescence organic carbon can have enormous applications. Research is being done to find a solution for the toxicity nature of obtained material, therefore the effectiveness of the non-toxic biopolymer is being examined for photoluminescence (Pan et al., 2014). Graph 6 provides the chitosan photoluminescence spectrum. It can be seen from the spectra that chitosan has a substantially higher photoluminescence intensity. Chitosan has an excitation wavelength of 434nm and an emission





Annlin Bezy et al.,

wavelength in 594 nm, which comes in the green shift. According to the PL spectrum, calculated the energy gap is 2.08eV.

CONCLUSION

Chitosan was successfully and inexpensively extracted through the chemical method from shrimp shell waste collected from the food processing industry. XRD and FTIR analysis was performed for the obtained chitosan. FTIR examination reveals each of the chitosan bonds is observed in the spectrum. XRD pattern shows the chitosan's crystallinity and grain size as 6.09 nm. In SEM, the uniformly distributed porous surface morphology throughout with rhombus shape is seen and considered as a better application result. The EDAX result is proved by spectra since it relates to the elements required for the formation of chitosan's polysaccharide chains. The optical examination of photoluminescence produced highly intense emission wavelengths in the region of the green shift. The measured energy difference between the extracted chitosan's excitation and emission wavelength was 2.08eV. The material obtained with good morphology is a unique result suggesting the extracted chitosan which is non-toxic, biodegradable, and biocompatible for adsorbent applications.

REFERENCES

1. Arafat A, Sabrin A Samad, Shah Md. Masum, & Mohammad Moniruzzaman. (2015). Preparation and Characterization of Chitosan from Shrimp shell waste. *International Journal of Scientific & Engineering Research*, 6(5), 538–541.
2. Bantz, C., Koshkina, O., Lang, T., Galla, H.-J., Kirkpatrick, C. J., Stauber, R. H., & Maskos, M. (2014). The surface properties of nanoparticles determine the agglomeration state and the size of the particles under physiological conditions. *Beilstein Journal of Nanotechnology*, 5, 1774–1786. <https://doi.org/10.3762/bjnano.5.188>
3. Baxter, A., Dillon, M., Anthony Taylor, K. D., & Roberts, G. A. F. (1992). An improved method for i.r. determination of the degree of N-acetylation of chitosan. *International Journal of Biological Macromolecules*, 14(3), 166–169. [https://doi.org/10.1016/S0141-8130\(05\)80007-8](https://doi.org/10.1016/S0141-8130(05)80007-8)
4. Bhullar, N., Rani, S., Kumari, K., & Sud, D. (2021). Amphiphilic chitosan/acrylic acid/thiourea based semi-interpenetrating hydrogel: Solvothermal synthesis and evaluation for controlled release of an organophosphate pesticide, triazophos. *Journal of Applied Polymer Science*, 138(25), 50595. <https://doi.org/10.1002/app.50595>
5. de Alvarenga, E. S. (2011). Characterization and Properties of Chitosan. In *Biotechnology of Biopolymers*. InTech. <https://doi.org/10.5772/17020>
6. Deepthi, S., Venkatesan, J., Kim, S.-K., Bumgardner, J. D., & Jayakumar, R. (2016). An overview of chitin or chitosan/nano ceramic composite scaffolds for bone tissue engineering. *International Journal of Biological Macromolecules*, 93, 1338–1353. <https://doi.org/10.1016/j.ijbiomac.2016.03.041>
7. Dokhaee, Z., Maghsoudi, A., Ghiaci, P., & Ghiaci, M. (2019). Investigation of the blends of chitosan and tragacanth as potential drug carriers for the delivery of ibuprofen in the intestine. *New Journal of Chemistry*, 43(37), 14917–14927. <https://doi.org/10.1039/C9NJ03617B>
8. Kumari, S., Kumar Annamareddy, S. H., Abanti, S., & Kumar Rath, P. (2017). Physicochemical properties and characterization of chitosan synthesized from fish scales, crab, and shrimp shells. *International Journal of Biological Macromolecules*, 104, 1697–1705. <https://doi.org/10.1016/j.ijbiomac.2017.04.119>
9. Nasrazadani, S., & Hassani, S. (2016). Modern analytical techniques in failure analysis of aerospace, chemical, and oil and gas industries. In *Handbook of Materials Failure Analysis with Case Studies from the Oil and Gas Industry* (pp. 39–54). Elsevier. <https://doi.org/10.1016/B978-0-08-100117-2.00010-8>
10. Pan, X., Ren, W., Gu, L., Wang, G., & Liu, Y. (2014). Photoluminescence from Chitosan for Bio-Imaging. *Australian Journal of Chemistry*, 67(10), 1422. <https://doi.org/10.1071/CH14274>
11. Ross Hallett, F. (1994). Particle size analysis by dynamic light scattering. *Food Research International*, 27(2), 195–198. [https://doi.org/10.1016/0963-9969\(94\)90162-7](https://doi.org/10.1016/0963-9969(94)90162-7)





Annlin Bezy et al.,

12. Sagheer, F. A. al, Al-Sughayer, M. A., Muslim, S., &Elsabee, M. Z. (2009). Extraction and characterization of chitin and chitosan from marine sources in the Arabian Gulf. *Carbohydrate Polymers*, 77(2), 410–419. <https://doi.org/10.1016/j.carbpol.2009.01.032>
13. Sakho, E. H. M., Allahyari, E., Oluwafemi, O. S., Thomas, S., &Kalarikkal, N. (2017). Dynamic Light Scattering (DLS). In *Thermal and Rheological Measurement Techniques for Nanomaterials Characterization* (pp. 37–49). Elsevier. <https://doi.org/10.1016/B978-0-323-46139-9.00002-5>
14. Singh, N., &Chahar, S. (2021). *Synthesis and characterization of chitosan prepared from shrimp shell*. 6, 296–300.
15. Thein-Han, W. W., Saikhun, J., Pholpramoo, C., Misra, R. D. K., &Kitiyanant, Y. (2009). Chitosan–gelatin scaffolds for tissue engineering: Physico-chemical properties and biological response of buffalo embryonic stem cells and transfectant of GFP–buffalo embryonic stem cells. *Acta Biomaterialia*, 5(9), 3453–3466. <https://doi.org/10.1016/j.actbio.2009.05.012>
16. Trung, T. S., Thein-Han, W. W., Qui, N. T., Ng, C.-H., & Stevens, W. F. (2006). Functional characteristics of shrimp chitosan and its membranes as affected by the degree of deacetylation. *Bioresource Technology*, 97(4), 659–663. <https://doi.org/10.1016/j.biortech.2005.03.023>
17. Wang, M., Shen, J., Thomas, J. C., Mu, T., Liu, W., Wang, Y., Pan, J., Wang, Q., & Liu, K. (2021). Particle Size Measurement Using Dynamic Light Scattering at Ultra-Low Concentration Accounting for Particle Number Fluctuations. *Materials*, 14(19), 5683. <https://doi.org/10.3390/ma14195683>
18. Xu, R. (2015). Light scattering: A review of particle characterization applications. *Particuology*, 18, 11–21. <https://doi.org/10.1016/j.partic.2014.05.002>
19. Younes, I., Hajji, S., Frachet, V., Rinaudo, M., Jellouli, K., & Nasri, M. (2014). Chitin extraction from shrimp shell using enzymatic treatment. Antitumor, antioxidant, and antimicrobial activities of chitosan. *International Journal of Biological Macromolecules*, 69, 489–498. <https://doi.org/10.1016/j.ijbiomac.2014.06.013>
20. Zaboon, M., Saleh, A., & Al-Lami, H. (2019). Comparative Cytotoxicity and Genotoxicity Assessments of Chitosan Amino Acid Derivative Nanoparticles Toward Human Breast Cancer Cell Lines. *Egyptian Journal of Chemistry*, 0(0), 0–0. <https://doi.org/10.21608/ejchem.2019.10806.1708>

Table 1. XRD data of chitosan

Angle 2θ(Degree)	Rel. Intensity (%)	d Spacing (Å)	FWHM
9.3812	40	9.419	1.562
19.4976	100	4.549	2.147
23.5	17	3.782	1.48
26.3373	27	3.381	1.347

Table 2. Elemental analysis data of chitosan

Element	Weight%	Atomic %
C	13.61	43.11
N	6.6	17.93
O	16.38	38.96



